Catalase Therapy Corrects Oxidative Stress-Induced Pathophysiology in Incipient Diabetic Retinopathy

Courtney R. Giordano,[1] Robin Roberts,[2] Kendra A. Krentz,[1] David Bissig,[2] Deepa Talreja,[3] Ashok Kumar,[2,3] Stanley R. Terlecky,[1] and Bruce A. Berkowitz[2,3]

[1]Department of Pharmacology, Wayne State University, Detroit, Michigan, United States
[2]Department of Anatomy and Cell Biology, Wayne State University, Detroit, Michigan, United States
[3]Department of Ophthalmology, Wayne State University, Detroit, Michigan, United States

Correspondence: Bruce A. Berkowitz, Department of Anatomy and Cell Biology, Wayne State University School of Medicine, 540 E. Canfield, Detroit, MI 48201, USA;
baberko@med.wayne.edu.

Submitted: December 4, 2014
Accepted: March 18, 2015

Citation: Giordano CR, Roberts R, Krentz KA, et al. Catalase therapy corrects oxidative stress-induced pathophysiology in incipient diabetic retinopathy. *Invest Ophthalmol Vis Sci*. 2015;56:3095–3102.
DOI:10.1167/iovs.14-16194

Purpose. Preclinical studies have highlighted retinal oxidative stress in the pathogenesis of diabetic retinopathy. We evaluated whether a treatment designed to enhance cellular catalase reduces oxidative stress in retinal cells cultured in high glucose and in diabetic mice corrects an imaging biomarker responsive to antioxidant therapy (manganese-enhanced magnetic resonance imaging [MEMRI]).

Methods. Human retinal Müller and pigment epithelial cells were chronically exposed to normal or high glucose levels and treated with a cell-penetrating derivative of the peroxisomal enzyme catalase (called CAT-SKL). Hydrogen peroxide (H_2O_2) levels were measured using a quantitative fluorescence-based assay. For in vivo studies, streptozotocin (STZ)-induced diabetic C57Bl/6 mice were treated subcutaneously once a week for 3 to 4 months with CAT-SKL; untreated age-matched nondiabetic controls and untreated diabetic mice also were studied. MEMRI was used to analytically assess the efficacy of CAT-SKL treatment on diabetes-evoked oxidative stress-related pathophysiology in vivo. Similar analyses were performed with difluoromethylornithine (DFMO), an irreversible inhibitor of ornithine decarboxylase.

Results. After catalase transduction, high glucose-induced peroxide production was significantly lowered in both human retinal cell lines. In diabetic mice in vivo, subnormal intraretinal uptake of manganese was significantly improved by catalase supplementation. In addition, in the peroxisome-rich liver of treated mice catalase enzyme activity increased and oxidative damage (as measured by lipid peroxidation) declined. On the other hand, DFMO was largely without effect in these in vitro or in vivo assays.

Conclusions. This proof-of-concept study raises the possibility that augmentation of catalase is a therapy for treating the retinal oxidative stress associated with diabetic retinopathy.

Keywords: catalase, diabetes, retina, MEMRI, oxidative stress

Accumulating evidence supports diabetes-evoked rod-dominated retinal oxidative stress as a pathogenic factor in experimental diabetic retinopathy.[1–4] However, targeting such stress using conventional antioxidant treatment is complicated by the fact that reactive oxygen species (ROS) have a central role in a number of normal cellular activities, including endomembrane signaling cascades, communication networks, and metabolic regulatory complexes.[5] Here, we examine the effects of a peroxisome-targeted protein biologic on specific biomarkers associated with diabetic retinopathy.

The peroxisome is a critical, but understudied subcellular constituent that is involved in a number of important redox-based metabolic processes in the cell.[6,7] These peroxisomal reactions are significant contributors to the oxidative load in aged cells and in several degenerative diseases, including diabetes.[7,8] Peroxisomal ROS accumulates for a number of reasons including, perhaps most importantly, mislocalization or impaired activity of catalase, its major resident antioxidant enzyme.[7,9] Diabetes reduces whole retinal catalase levels, although a specific contribution of peroxisomes per se in diabetic retinopathy is unclear.[10–14] The goal of this study was to begin to determine if targeting cells with catalase supplementation could confer antioxidant protection in the context of diabetic retinopathy. To this end, we examined oxidative stress in retinal cells exposed to high glucose conditions, and determined if an in vivo biomarker sensitive to antioxidant treatment in diabetic models also was positively impacted by targeted catalase treatment.

In this feasibility study, hydrogen peroxide (H_2O_2) levels were first evaluated in retinal (Müller and RPE) cell lines chronically exposed to high glucose levels and treated with CAT-SKL, a cell penetrating catalase derivative designed to traffic to peroxisomes (described in a previous study[8] and references therein).

Polyamines, which include spermine, spermidine, and putrescine, are prevalent in the retina.[15] These molecules have been reported to possess, among other activities, antioxidant/radical scavenger action. Interestingly, polyamines also have been suggested to contribute to diabetes-induced oxidative stress in endothelial cells.[16] The latter effect may be mediated by increased activity of the H_2O_2-generating peroxisomal enzyme, polyamine oxidase. Indeed, in a clinical study, diabetes increased ocular polyamines raising the possibility of enhanced polyamine oxidase activity.[17] Thus, we examined the effects of

the polyamine synthesis inhibitor, difluoromethylornithine (DFMO), which demonstrates antioxidant benefits in certain contexts, but whose impact on diabetic retinopathy have yet to be described. Our study represents a first step in parsing the contributions of these different activities in diabetic retinopathy.

We also examined whether CAT-SKL or DFMO might be useful in vivo using manganese-enhanced magnetic resonance imaging (MEMRI), a noninvasive measurement of intraretinal uptake of manganese ion (Mn^{2+}, a strong MRI contrast agent) as an analytical biomarker of intraretinal calcium channel activity in the retina encoded while animals are awake and freely moving.[18–20] MEMRI recently has emerged as the imaging modality of choice when performing studies of retinal ion activity.[21] In diabetic rats and mice, reduced intraretinal uptake of manganese precedes the appearance of frank retinal histopathology.[22,23] Importantly, antioxidant therapies that correct these early MEMRI impairments also correct later diabetic retinopathy.[22,23] For these reasons, we used MEMRI to begin an analysis of CAT-SKL and DMFO's in vivo efficacies.

Here, we find that CAT-SKL reduced diabetes-evoked H_2O_2 production in retinal cells and partly improved the subnormal retinal uptake of manganese in vivo. On the other hand, DFMO showed no such effects on retinal cells or in our in vivo analyses. These results suggest the use of a targeted antioxidant, CAT-SKL, as a potential useful treatment against the oxidative stress associated with diabetic retinopathy.

Materials and Methods

All animals were treated in accordance with the National Institutes of Health (NIH; Bethesda, MD, USA) Guide for the Care and Use of Laboratory Animals, the Association for Research in Vision and Ophthalmology (ARVO) Statement for the Use of Animals in Ophthalmic and Vision Research, and Institutional Animal and Care Use Committee (IACUC) authorization. Animals were housed and maintained in normal 12-hour:12-hour light-dark cycle laboratory lighting, unless otherwise noted.

Cell Culture

Human retinal pigment epithelium (ARPE-19) cells were obtained from American Type Culture Collection (ATCC; Manassas, VA, USA). Spontaneously immortalized human Müller cells (MIO-M1) were a gift from G. Astrid Limb (University College London, London, UK) and were maintained as previously described.[24] The retinal cell lines were grown in Dulbecco's modified Eagle medium (DMEM; MIO-M1), or DMEM:Nutrient Mixture F-12 (DMEM:F12) (ARPE-19) with normal glucose (NG; 5 mM), or DMEM with high glucose (HG; 17.5 mM). Chronic NG or HG cells were acquired after 10 passages in media supplemented with either NG or HG concentrations.

CAT-SKL Transduction

We purified and characterized CAT-SKL as described previously.[8,25,26] To track entry into cells, the molecule was biotinylated on primary amines.[8,25] Cells were treated with biotinylated CAT-SKL (100 nM) for 0, 1, 2, and 4 hours at which time they were harvested into sample buffer. Proteins were separated by SDS-PAGE and then transferred to a nitrocellulose membrane. The membrane was blocked using 5% nonfat milk and probed with streptavidin-alkaline phosphatase (diluted 1:1000). Reactive proteins were visualized with the NBT/BCIP 1-Step Solution (Thermo Fisher Scientific, Inc., Waltham, MA, USA).

Catalase Activity

Catalase enzymatic activity was determined by its ability to decompose H_2O_2 as described previously.[27] Here, equal numbers of cells or equal tissue protein were added to 1 mg/mL BSA, 0.02 M imidazole (pH 7.0), 0.2% Triton X-100, 0.06% H_2O_2 (prepared fresh) in PBS, and the reaction incubated at room temperature for 15 minutes. Titanium oxysulfate stop solution then was added and resultant absorbance at 405 nm was measured on a microplate reader. Catalase transduction of Müller and RPE cells was accomplished by treating cells (or not) with 1 μM CAT-SKL for 24 hours. Confirmation of transduction was made by Western blot analysis. Cells were harvested in PBS, equal amounts of protein were separated by SDS and transferred to a nitrocellulose membrane. Antibodies used included anti-catalase and anti-β-actin, diluted 1:4000 and 1:10,000, respectively.

Measurement of H_2O_2

Müller and RPE cells were plated at 20,000 cells per well in 96-well plates, allowed to adhere for 24 hours and then treated with or without either 1 μM CAT-SKL or 5 mM DFMO for 24 hours at 37°C. Where indicated, heat inactivated CAT-SKL was prepared by boiling at 100°C for 3 minutes, cooling to room temperature, and resuspending as appropriate in cell culture media. The H_2O_2 levels were determined using the Amplex Red Hydrogen Peroxide/Peroxidase Assay Kit (Molecular Probes; Thermo Fisher Scientific, Inc.) following the manufacturer's protocol. Briefly, cells were washed with Hank's balanced salt solution, treated with the Amplex Red reagent (10-acetyl-3,7-dihydroxy-phenoxazine)/horseradish peroxidase working solution and incubated for 2 hours at room temperature protected from light. Fluorescence units were obtained using a microplate reader (excitation 544 nm and emission 590 nm). Background fluorescence in wells containing media alone was subtracted from all data points.

Mice

At 2 months of age, 20-g male C57Bl/6 mice (Jackson Laboratories, Bar Harbor, ME, USA) were randomly assigned into the following groups: nondiabetic age-matched controls, diabetics, diabetics with treatments (diabetic + CAT-SKL), and (diabetic + DFMO).

Diabetes

Diabetes was induced in mice with starting weights of 16 to 20g by streptozotocin (STZ), (60 mg/kg; 10 mM citrate buffer [pH 4.5]) intraperitoneal injection, within 10 minutes of preparation, once a day for 5 consecutive days. Body weight and blood glucose levels were monitored twice weekly. Insulin (neutral protamine Hagedorn, a type of insulin with an intermediate level of activity), Humulin N (Eli Lilly, Indianapolis, IN, USA; available in the public domain at lilly.com), administered to mice as needed based on bodyweight and blood glucose levels, but not more than twice weekly, allowed slow weight gain while maintaining hyperglycemia (blood glucose levels higher than 400 mg/dL). Mice that lost weight and/or had blood glucose levels greater than 600 mg/dL were given 0.1 to 0.2 units of Lilly Humulin N insulin. Normal rodent chow (Purina TestDiet 5001; Purina, Richmond, IN, USA), which contains 11.2% fat, 26% protein, and 62.7% carbohydrate, and water were provided ad libitum. Dehydrated animals were administered saline as needed. Hemoglobin A1c was measured (Glyco-Tek affinity columns, kit 5351; Helena Laboratories, Beaumont, TX, USA) from blood collected after

Investigative Ophthalmology & Visual Science

each MEMRI experiment. Blood was drawn from the left ventricle, after puncture, into a capillary tube and stored in an Eppendorf tube with a small amount of heparin to prevent coagulation. The blood was kept at 4°C until analysis within 1 week following the MEMRI experiment.

CAT-SKL Treatment

A random subset of diabetic mice were treated subcutaneously with CAT-SKL (1 mg/kg) weekly for 3 to 4 months, starting 1 week after initiation and confirmation of the diabetic state. Two treated diabetic mice had relatively low A1c values (8.6% and 8.9%) and were excluded from the final analysis. Our rationale was to exclude effects that might be due to improved serum glucose control. Note that the control and diabetic mice data have been reported in a previous study.[28] At the end of the 4-month study period, untreated controls ($n = 7$), diabetic animals ($n = 7$), and diabetic animals treated with CAT-SKL ($n = 5$) underwent MEMRI examination.

DFMO Treatment

In the chronic hyperglycemia groups, mice were maintained as diabetic for 3 to 5 months. Difluoromethylornithine (kind gift from Patrick Woster, Wayne State University [Detroit, MI, USA], now at Medical College of South Carolina [Charleston, SC, USA]) was administered at a dose of 1% (wt/vol) in the water for 1 week before MEMRI examination. At the end of the study period, untreated controls ($n = 13$), diabetic animals ($n = 7$), and diabetic animals treated with DFMO ($n = 7$) were examined by MEMRI.

Tissue Protein Extraction

Tissue (500 mg/mL) was homogenized on ice in a Dounce homogenizer in tissue protein extraction buffer (50 mM Tris-HCL, pH 7.8, 150 mM NaCl, 1 mM DTT, 0.1% Tween-20, and protease inhibitor cocktail [Thermo Fisher Scientific, Inc.]). The sample volume was transferred to an Eppendorff tube and spun at 20,000*g* at 4°C for 20 minutes and repeated one time. The resulting supernatant was the sample used for lipid hydroperoxide and catalase measurements.

Lipid Hydroperoxide Measurements

Lipid hydroperoxide levels were measured in mouse livers following the manufacturer's protocol (catalog #70500; Cayman Chemical, Ann Arbor, MI, USA).

MEMRI Measurement

The methodologies for measuring MEMRI in mice have been described in detail previously.[28] Briefly, all animals were maintained in darkness for 16 to 20 hours before manganese injection. All procedures (i.e., weighing, injecting $MnCl_2$, anesthetic administration, and MRI examination) were performed under dim red light or darkness. Mangaese chloride ($MnCl_2$) was administered as an intraperitoneal injection (66 mg $MnCl_2 \bullet 4H_2O$/kg) on the right side of the awake animal. After this injection, animals were maintained in dark conditions for another 3.5 to 4 hours. Immediately before the MRI experiment, animals were anesthetized with urethane (36% solution intraperitoneally; 0.083 mL/20 g animal weight, prepared fresh daily; Aldrich, Milwaukee, WI, USA). The MRI data were acquired on a 7T system (Clinscan; Bruker Corporation, Billerica, MA, USA). Retinal partial saturation T_1 data were acquired using a dual coil mode on a 7 T Bruker Clinscan system: Several single spin-echo (time to echo [TE] 13 ms, 7×7 mm^2, matrix size 160×320, slice thickness 600 μm) images were acquired at different repetition times [TRs] in the following order (number per time between repetitions in parentheses): TR 0.15 seconds (6), 3.50 seconds (1), 1.00 seconds (2), 1.90 seconds (1), 0.35 seconds (4), 2.70 seconds (1), 0.25 seconds (5), and 0.50 seconds (3). To compensate for reduced signal-noise ratios at shorter TRs, progressively more images were collected as the TR decreased.

MRI Analysis

The MEMRI data of central retinal results (±1 mm from the center of the optic nerve) were analyzed using the region-of-interest. The white box region-of-interest indicates the part of central retina (including optic nerve [ON]) that was linearized for the control, untreated diabetic and treated diabetic (diabetic + CAT-SKL) groups. Quantitative analysis was as follows: single images acquired with the same TR were first registered (rigid body) and then averaged. These averaged images then were registered across TRs. The same regions-of-interest as above were analyzed by calculating $1/T_1$ maps by first fitting to a three-parameter T_1 equation ($y = a + b^*[\exp(-c^*TR)]$, where a, b, and c are fitted parameters) on a pixel-by-pixel basis using R (v.2.9.0, R Development Core Team, R: A language and environment for statistical computing, R Foundation for Statistical Computing, ISBN 3–900051–07–0, available in the public domain at http://www.r-project.org/) scripts developed in-house, and the minpack.lm package (v.1.1.1, Timur V. Elzhov and Katharine M. Mullen minpack.lm: R interface to the Levenberg-Marquardt nonlinear least-squares algorithm found in MINPACK. R package version 1.1–1). The reciprocal ($1/T_1$) values directly reflect manganese levels. Central intraretinal $1/T_1$ profiles were obtained as detailed previously.[29] Values from the superior and inferior retina were averaged. Note that only those animals that took up manganese above baseline (i.e., ~0.6 s^{-1}) were included in the final analysis. The present resolution in the central retina is sufficient for extracting meaningful layer-specific anatomical and functional data, as discussed previously.[30,31] In these studies, whole-retinal thicknesses in C mice was approximately 220 μm studied with an axial pixel size of 25 μm.[30] We note that the spatial uncertainty is approximately one-half-pixel thick (~12.5 μm).[30] These considerations also support our ability to distinguish significant uptake differences within the retina. In all cases, animals were humanely euthanized as detailed in our IACUC-approved protocol.

Statistical Analysis

Statistical analysis on drug-treated versus untreated cell culture values were performed using GraphPad Prism version 5.0 (GraphPad Software, Inc., La Jolla, CA, USA). Student's *t*-tests were used to compare two groups and 1-way ANOVA was used to compare three or more groups. Where ANOVA indicated significance, means were separated using Tukey's Multiple Comparison Test. Comparisons of MEMRI data between groups were performed using individual *t*-tests at different locations of the intraretinal profiles. Comparisons of MEMRI retinal signal intensities were performed using a generalized estimating equation (GEE) approach.[18,32] GEE performs a general linear regression analysis using all of the pixels in each subject and accounts for the within-subject correlation between adjacent pixels. GEE was performed using the GENMOD procedure in SAS for windows with the working correlation matrix set to autoregressive (1) and the scale parameter set to the Pearson χ^2. In all cases, $P < 0.05$ was considered statistically significant.

Investigative Ophthalmology & Visual Science

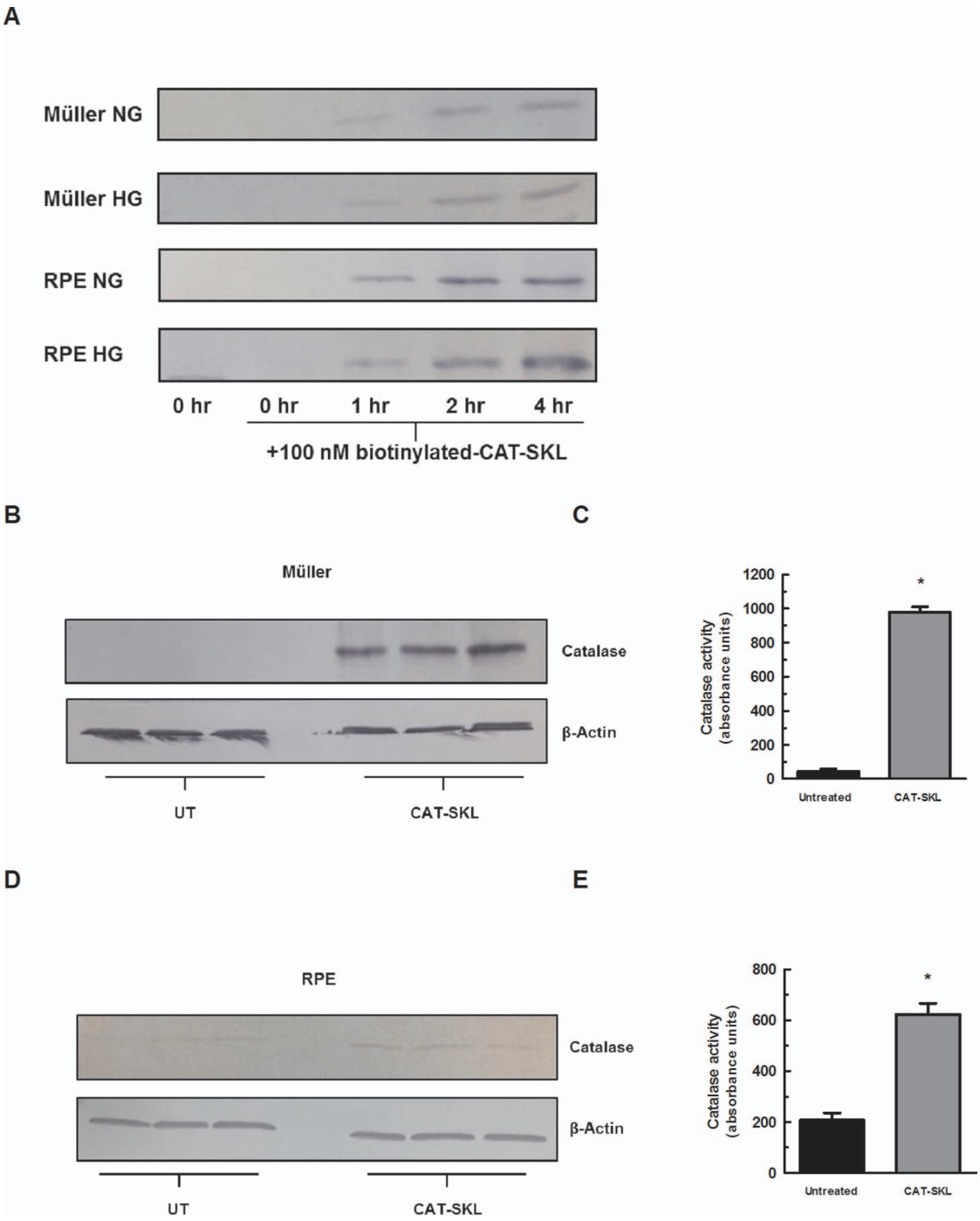

Figure 1. CAT-SKL transduction of retinal cells. (**A**) Müller and RPE cells were cultured in NG (5 mM) or HG (17.5 mM) media as indicated. The cells were treated for 0, 1, 2, and 4 hours with biotinylated CAT-SKL (100 nM), washed, and harvested. Transduction efficacy was assessed by Western blotting. *Bands* shown migrate at position expected for CAT-SKL. Müller (**B**, **C**) and RPE (**D**, **E**) cells were transduced with 1 μM CAT-SKL (indicated as "CAT-SKL") or without (indicated as "UT") for 24 hours, washed, and harvested in PBS. Equal amounts of protein were separated by SDS-PAGE and probed with anti-catalase and anti-β-actin antibodies or catalase activity was measured enzymatically (*$P < 0.05$).

Results

Cell Culture

First, we confirmed CAT-SKL bioavailability in retinal cells. Müller and RPE cell lines in normal and high glucose media conditions were treated with biotinylated CAT-SKL for 0, 1, 2, and 4 hours. Transduction was observed within 1 hour of incubation (Fig. 1A). To confirm that transduced CAT-SKL increases cellular catalase, the protein was measured in Müller and RPE cells by SDS-PAGE and then immunoblotted (Figs. 1B, 1D). In addition, the activity of catalase was measured enzymatically showing a significant increase in catalase activity when treated with 1 μM CAT-SKL for 24 hours (Figs. 1C, 1E.) Müller and RPE cell lines cultured with chronically HG concentrations demonstrated an increase in H_2O_2 levels compared to those cultured in NG conditions (Figs. 2A, 2B). Importantly, supplementing cellular catalase with CAT-SKL was

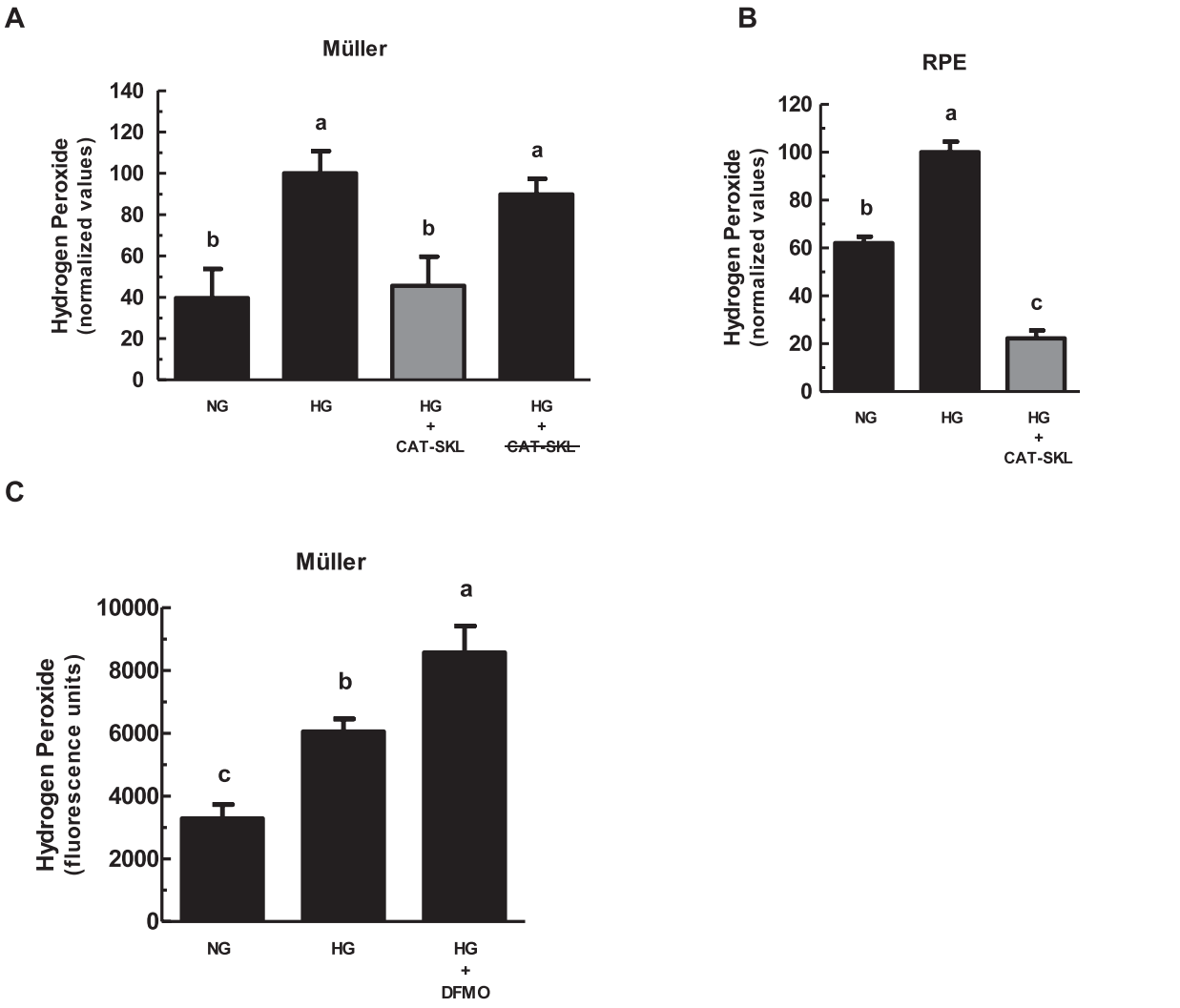

Figure 2. Enzymatically-active CAT-SKL reduces H_2O_2 levels in Müller and RPE cells. Müller (**A**, **C**) and RPE (**B**) cells were cultured over several passages in NG (5 mM) or HG (17.5 mM) media. Replicate cultures of HG cells then were treated with either 1 μM CAT-SKL or 5 mM DFMO for 24 hours as indicated. Hydrogen peroxide levels were measured using the Amplex Red reagent (10-acetyl-3,7-dihydroxyphenoxazine) assay kit. Results presented, means ± 1 SD of four or more samples, are normalized (**A**, **B**) to the HG value (arbitrarily set at 100). (**A**) Cells also were transduced with 1 μM enzymatically-inactive (heat denatured) CAT-SKL (indicated as CAT-SKL). *Error bars* represent mean ± SEM for quadruplicate samples. Means followed by the same letter are not significantly different according to Tukey's multiple comparison test ($P > 0.05$).

found to prevent supernormal peroxide buildup in both cell lines (Fig. 2). Furthermore, enzymatically inactive CAT-SKL elicited no significant effect on cellular H_2O_2 levels (Fig. 2A). Similar results were obtained with RPE cells cultured on filtered transwell plates (data not shown). Because Müller cells demonstrated the greatest range in oxidative stress between normal and high glucose conditions we limited our investigation of a potential antioxidant effect of DFMO to these cells. Previous studies have offered conflicting results on polyamines' neuroprotective effects and their role in aging and disease.[33,34] In contrast to CAT-SKL's protective effects against H_2O_2 in retinal cells, treatment with 5 mM DFMO had no such antioxidant properties and slightly increased H_2O_2 levels compared to HG conditions (Fig. 2C) in Müller cells.

In addition to measuring catalase and hyperglycemic-induced H_2O_2 in cells, catalase enzymatic activity and lipid peroxidation was evaluated in postmortem tissue. Figure 3A demonstrates an increase of lipid peroxidation in mouse livers of diabetic treated mice compared to controls. Importantly, treatment of diabetic mice with CAT-SKL (for 3 months) reduced lipid peroxidation levels in liver. Catalase enzyme activity also was decreased in diabetic mouse livers and rebounded when CAT-SKL was administered to diabetic mice (Fig. 3B). These results suggest that supplementing cellular catalase is an effective treatment for reducing levels of hyperglycemia-evoked H_2O_2 in retinal cells and in tissue.

Model Characteristics

Glycated hemoglobin (A1c) was examined in all groups and as expected for the diabetic mouse model, the A1c range was lower ($P < 0.05$) in age-matched nondiabetic controls (5.3%–7.0%) compared to either the nontreated diabetic animals (12.0%–14.4%) or the treated diabetic mice (10.9%–15.7%: no differences in A1c between diabetic groups were found ($P > 0.05$). The ranges of body weights also were different between age-matched nondiabetic controls (30–36 g) and untreated (17–23 g) and treated (18–23 g) diabetic groups; again the three diabetic groups did not differ ($P > 0.05$) in their final body weight.

Having established the usefulness of CAT-SKL as an effective antioxidant in retinal cells and postmortem nonretinal tissue,

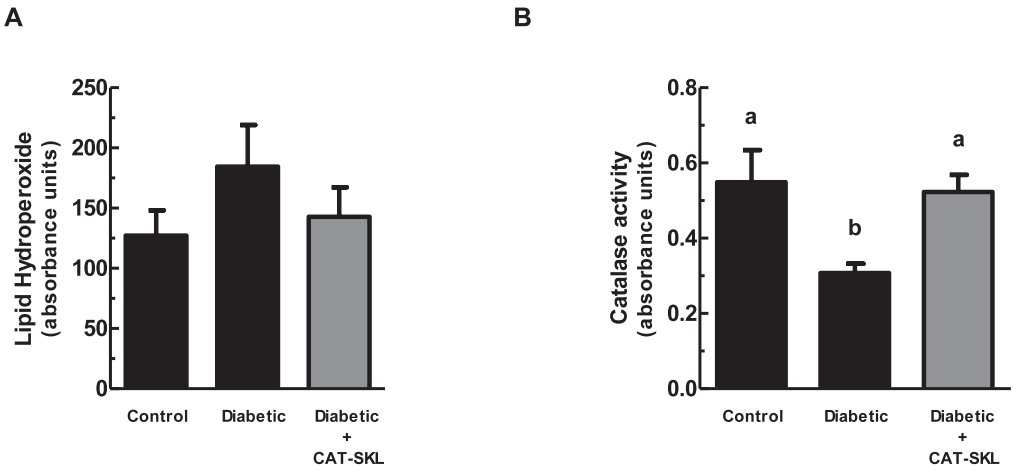

Figure 3. CAT-SKL reduces lipid hydroperoxide levels and increases catalase activity in tissue. (**A**) Lipid hydroperoxide levels were measured in mouse livers ($n = 4$) using the lipid hydroperoxide assay kit as described in the Materials and Methods. (**B**) Catalase activity was measured enzymatically in mouse liver as described in the Materials and Methods. *Error bars* represent mean ± SEM for quadruplicate samples. Means designated by different letters are significantly different ($P < 0.05$) according to Tukey's multiple comparison test.

we next asked about CAT-SKL's effectiveness in modulating retinal function in vivo.

MEMRI Measurements

Previously we reported on an antioxidant-sensitive early diabetes-evoked metric: decreased intraretinal manganese uptake as measured by MEMRI.[22,23] As summarized in Figure 4A, CAT-SKL treatment significantly ($P < 0.05$) improved uptake in the inner and outer retina. Treatment with DFMO did not correct any of the diabetes-induced MEMRI abnormalities (Fig. 4B).

Discussion

In this study, we found for the first time evidence that treatment with a cell penetrating catalase molecule (CAT-SKL) significantly corrected hyperglycemia-induced oxidative stress in retinal cells and nonretinal tissue as well as improved early oxidative stress-sensitive ion channel dysregulation in diabetic retinopathy in vivo. The present studies take advantage of the recent availability of CAT-SKL to begin to test for a contribution of peroxisomal oxidative stress to diabetic retinopathy. Importantly, treatment with the polyamine synthesis inhibitor, DFMO, had no such effects, suggesting this drug lacked broad effects on cellular antioxidant capacities. It is now clear that retinal oxidative stress is a pathogenic factor in diabetic retinopathy, based, in part, on previous studies using a variety of nonspecific/nontargeted antioxidants, all of which prevented the development of the pathology.[3,4,11,35,36] Questions remain, however, as to how antioxidants are best introduced into the retina with minimal perturbation of normal cellular functions. Brief and often continuous oxidative bursts are critical controllers of endomembrane signaling, inter- and intracellular communication networks, and coordinated metabolic regulation.[5] The results in this study raise the possibility that targeting peroxisomal oxidative stress is a novel and effective treatment strategy for diabetic retinopathy.

MEMRI is a powerful and sensitive assay to document beneficial effects of antioxidant strategies designed to treat early diabetes-evoked retinal pathophysiology.[22,23,37,38] For example, we previously reported that α-lipoic acid effectively reversed the subnormal intraretinal manganese uptake (mea-

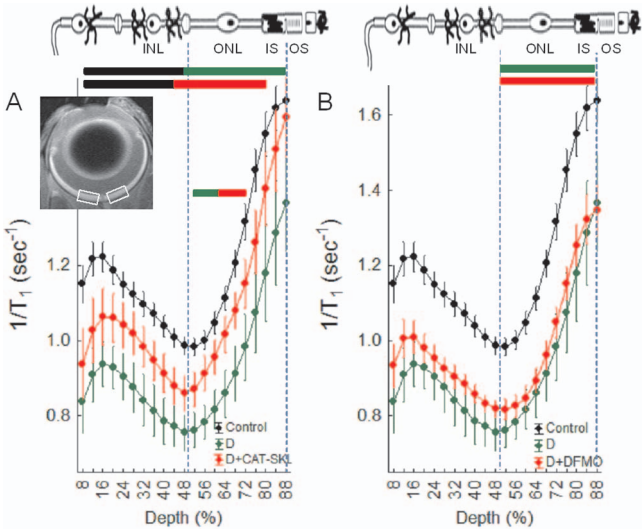

Figure 4. Impaired manganese uptake in the retina of diabetic mice is partially corrected with the targeted antioxidant CAT-SKL but not DFMO. (**A**) Summary of central retinal manganese uptake (i.e., $1/T_1$) in central retina (indicated by the *white boxes* in the *inset*) as a function of retinal depth in dark adapted wt controls (*black*), untreated diabetics (*green*), and CAT-SKL–treated diabetics (*red*) mice. Data are shown as a function of distance from the retina/nonretina borders, where 0% is the vitreous/retina border and 100% is the retina/choroid border. Regions near borders (<8% and >88% depth) are not shown because these regions likely include some signal from outside of the retina (i.e., partial volume averaging with vitreous or choroid/sclera). *Bicolored lines* above profiles indicate retinal regions with significant ($P < 0.05$) differences in manganese uptake between control and experimental mice indicated by the color. *Above graph*: Simplified schematic of retina and support circulations.[46–48] The retina has a well-defined laminar structure that allows us to reasonably label regions of uptake at 8% to 24% depth as the ganglion cell layer, 24% to 50% depth as the inner nuclear layer, 50% to 68% depth as rod nuclei, 68% to 80% depth as the rod inner segment region, and >80% as the rod outer segment region. *Error bars* represent standard error of the mean (SEM). No manganese baseline values were $0.6 s^{-1}$. (**B**) Summary of central retinal manganese uptake as a function of retinal depth in dark adapted wt controls (*black*, same data as in [**A**]), untreated diabetics (*green*, same data as in [**A**]), and DMO-treated diabetics (*red*) mice. This graph is presented using the same conventions as in (**A**).

Investigative Ophthalmology & Visual Science

sured by MEMRI) in diabetic rats.[22] Furthermore, we have also showed that overexpression of the copper/zinc binding antioxidant, superoxide dismutase, dramatically impacted diabetes-induced early MEMRI lesions and later retinopathy in diabetic mice.[23] MEMRI is a noninvasive technique that measures retinal open/closed status of L-type voltage gated calcium ion channels, crucial components of intracellular communication.[37–43] While it is not yet clear how retinal oxidative stress (due to diabetes) leads to impaired intraretinal uptake on MEMRI, our previous studies underscore the usefulness of the technique as providing a sensitive surrogate for antioxidant efficacy, a conclusion supported by the CAT-SKL data included herein.

This proof-of-concept study had one primary limitation. For technical reasons, we were unable to measure the effects of the CAT-SKL treatment on retinal oxidative stress. This limit is somewhat offset by our data showing that CAT-SKL was effective in retina cell cultures, nonretinal tissue, and on MEMRI examination. These data support our overriding hypothesis. We also found an incomplete correction of the diabetes-induced subnormal MEMRI retinal profiles that may reflect suboptimal CAT-SKL dosing. The fact that others have demonstrated catalase gene delivery to the RPE is protective against light damage[44] supports this latter point. A more thorough dose-response analysis clearly is warranted, which will allow us to more completely assess the protein therapeutic with regards to retinal ROS and diabetic retinopathy.

The pathogenesis of diabetic retinopathy is not completely understood, although there is strong consensus that increased rod-dominant retinal oxidative stress is a major contributor.[1,3,4,11,35,36] There are several potential ways in which rod cell oxidative stress in diabetic mice could be generated, including impaired activity of the major antioxidant defense enzymes—catalase and/or superoxide dismutase,[11,13] among others. Also, because in this study we found improvements in inner and outer retina, it is intriguing that the photoreceptor inner segments contain at least 60% to 65% of retinal mitochondria and are the primary retinal region that immunostains for catalase (and presumably peroxisomes).[45] Perhaps improvements in outer retinal oxidative stress lead to downstream improvements in inner retina oxidative stress.[1] To the best of our knowledge, treatment targeted to increasing peroxisomal catalase levels alone has not been investigated in diabetic retinopathy. The present findings raise the possibility that such highly specific supplementation of the powerful antioxidant enzyme will be useful in this debilitating disease.

Acknowledgments

We thank Timothy Kern (Case Western Reserve University, Cleveland, OH, USA) for helpful discussions, and Nick Davis and Ray Mattingly (Wayne State University, Detroit, MI, USA) for their helpful comments regarding the manuscript.

Supported by NIH Animal Models of Diabetic Complications Consortium and Mouse Metabolic Phenotyping Centers Pilot and Feasibility Programs (BAB); NIH Grant EY-19888 (AK); an unrestricted grant from Research to Prevent Blindness (Kresge Eye Institute, Detroit, MI, USA: Wayne State University School of Medicine MD/PhD Program [DB]); and NIH Grant AG034752 (DB). Development of CAT-SKL was supported in part by NIH Grant DK56299 (SRT).

Disclosure: **C.R. Giordano**, None; **R. Roberts**, None; **K.A. Krentz**, None; **D. Bissig**, None; **D. Talreja**, None; **A. Kumar**, None; **S.R. Terlecky**, EXT Life Sciences, Inc. (F, I, E, S), P; **B.A. Berkowitz**, None

References

1. Du Y, Veenstra A, Palczewski K, Kern TS. Photoreceptor cells are major contributors to diabetes-induced oxidative stress and local inflammation in the retina. *Proc Natl Acad Sci U S A*. 2013;110:16586–16591.
2. Kowluru RA, Atasi L, Ho YS. Role of mitochondrial superoxide dismutase in the development of diabetic retinopathy. *Invest Ophthalmol Vis Sci*. 2006;47:1594–1599.
3. Kowluru RA, Kowluru V, Xiong Y, Ho YS. Overexpression of mitochondrial superoxide dismutase in mice protects the retina from diabetes-induced oxidative stress. *Free Rad Biol Med*. 2006;41:1191–1196.
4. Kanwar M, Chan PS, Kern TS, Kowluru RA. Oxidative damage in the retinal mitochondria of diabetic mice: possible protection by superoxide dismutase. *Invest Ophthalmol Vis Sci*. 2007;48:3805–3811.
5. Lee J, Giordano S, Zhang J. Autophagy, mitochondria and oxidative stress: cross-talk and redox signalling. *Biochem J*. 2012;441:523–540.
6. Ivashchenko O, Van Veldhoven PP, Brees C, Ho YS, Terlecky SR, Fransen M. Intraperoxisomal redox balance in mammalian cells: oxidative stress and interorganellar cross-talk. *Mol Biol Cell*. 2011;22:1440–1451.
7. Terlecky SR, Terlecky LJ, Giordano CR. Peroxisomes, oxidative stress, and inflammation. *World J Biol Chem*. 2012;3:93–97.
8. Giordano CR, Terlecky SR. Peroxisomes, cell senescence, and rates of aging. *Biochim Biophys Acta*. 2012;1822:1358–1362.
9. Terlecky SR, Koepke JI, Walton PA. Peroxisomes and aging. *Biochim Biophys Acta*. 2006;1763:1749–1754.
10. Zhang H, Agardh CD, Agardh E. Retinal nitro blue tetrazolium staining and catalase activity in rat models of diabetes. *Graefes Arch Klin Exp Ophthalmol*. 1996;234:324–330.
11. Kowluru RA, Kern TS, Engerman RL. Abnormalities of retinal metabolism in diabetes or experimental galactosemia. IV. Antioxidant defense system. *Free Rad Biol Med*. 1997;22:587–592.
12. Kocak G, Aktan F, Canbolat O, et al. Alpha-lipoic acid treatment ameliorates metabolic parameters, blood pressure, vascular reactivity and morphology of vessels already damaged by streptozotocin-diabetes. *Diab Nutr Metab*. 2000;13:308–318.
13. Obrosova IG, Drel VR, Kumagai AK, Szabo C, Pacher P, Stevens MJ. Early diabetes-induced biochemical changes in the retina: comparison of rat and mouse models. *Diabetologia*. 2006;49:2525–2533.
14. Sadi G, Yilmaz O, Guray T. Effect of vitamin C and lipoic acid on streptozotocin-induced diabetes gene expression: mRNA and protein expressions of Cu-Zn SOD and catalase. *Mol Cell Biochem*. 2008;309:109–116.
15. Biedermann B, Skatchkov SN, Brunk I, et al. Spermine/spermidine is expressed by retinal glial (Muller) cells and controls distinct K+ channels of their membrane. *Glia*. 1998;23:209–220.
16. Ishizaki E, Fukumoto M, Puro DG. Functional K(ATP) channels in the rat retinal microvasculature: topographical distribution, redox regulation, spermine modulation and diabetic alteration. *J Physiol*. 2009;587:2233–2253.
17. Nicoletti R, Venza I, Ceci G, Visalli M, Teti D, Reibaldi A. Vitreous polyamines spermidine, putrescine, and spermine in human proliferative disorders of the retina. *Br J Ophthalmol*. 2003;87:1038–1042.
18. Berkowitz BA, Roberts R, Goebel DJ, Luan H. Noninvasive and simultaneous imaging of layer-specific retinal functional adaptation by manganese-enhanced MRI. *Invest Ophthalmol Vis Sci*. 2006;47:2668–2674.
19. Berkowitz BA, Gradianu M, Schafer S, et al. Ionic dysregulatory phenotyping of pathologic retinal thinning with manganese-

enhanced MRI. *Invest Ophthalmol Vis Sci*. 2008;49:3178–3184.

20. Berkowitz BA, Roberts R, Oleske DA, et al. Quantitative mapping of ion channel regulation by visual cycle activity in rodent photoreceptors in vivo. *Invest Ophthalmol Vis Sci*. 2009;50:1880–1885.
21. Ramos de Carvalho JE, Verbraak FD, Aalders MC, van Noorden CJ, Schlingemann RO. Recent advances in ophthalmic molecular imaging. *Surv Ophthalmol*. 2014;59:393–413.
22. Berkowitz BA, Roberts R, Stemmler A, Luan H, Gradianu M. Impaired apparent ion demand in experimental diabetic retinopathy: correction by lipoic Acid. *Invest Ophthalmol Vis Sci*. 2007;48:4753–4758.
23. Berkowitz BA, Gradianu M, Bissig D, Kern TS, Roberts R. Retinal ion regulation in a mouse model of diabetic retinopathy: natural history and the effect of Cu/Zn superoxide dismutase overexpression. *Invest Ophthalmol Vis Sci*. 2009;50:2351–2358.
24. Shamsuddin N, Kumar A. TLR2 mediates the innate response of retinal Muller glia to Staphylococcus aureus. *J Immunol*. 2011;186:7089–7097.
25. Koepke JI, Nakrieko KA, Wood CS, et al. Restoration of peroxisomal catalase import in a model of human cellular aging. *Traffic*. 2007;8:1590–1600.
26. Young CN, Koepke JI, Terlecky LJ, Borkin MS, Boyd Savoy L, Terlecky SR. Reactive oxygen species in tumor necrosis factor-alpha-activated primary human keratinocytes: implications for psoriasis and inflammatory skin disease. *J Invest Dermatol*. 2008;128:2606–2614.
27. Storrie B, Madden EA. Isolation of subcellular organelles. *Methods Enzymol*. 1990;182:203–225.
28. Berkowitz BA, Bissig D, Patel P, Bhatia A, Roberts R. Acute systemic 11-cis-retinal intervention improves abnormal outer retinal ion channel closure in diabetic mice. *Mol Vis*. 2012;18:372–376.
29. Bissig D, Berkowitz BA. Same-session functional assessment of rat retina and brain with manganese-enhanced MRI. *NeuroImage*. 2011;58:749–760.
30. Berkowitz BA, Grady EM, Khetarpal N, Patel A, Roberts R. Oxidative stress and light-evoked responses of the posterior segment in a mouse model of diabetic retinopathy. *Invest Ophthalmol Vis Sci*. 2015;56:606–615.
31. Berkowitz BA, Grady EM, Roberts R. Confirming a prediction of the calcium hypothesis of photoreceptor aging in mice. *Neurobiol Aging*. 2014;35:1883–1891.
32. Zeger SL, Liang KY. Longitudinal data analysis for discrete and continuous outcomes. *Biometrics*. 1986;42:121–130.
33. von Deutsch AW, Mitchell CD, Williams CE, et al. Polyamines protect against radiation-induced oxidative stress. *Grav Space Biol Bull*. 2005;18:109–110.
34. Minois N, Carmona-Gutierrez D, Madeo F. Polyamines in aging and disease. *Aging*. 2011;3:716–732.
35. Kowluru RA, Kern TS, Engerman RL, Armstrong D. Abnormalities of retinal metabolism in diabetes or experimental galactosemia. III. Effects of antioxidants. *Diabetes*. 1996;45:1233–1237.
36. Kowluru RA, Tang J, Kern TS. Abnormalities of retinal metabolism in diabetes and experimental galactosemia. VII. Effect of long-term administration of antioxidants on the development of retinopathy. *Diabetes*. 2001;50:1938–1942.
37. Marmorstein LY, Wu J, McLaughlin P, et al. The light peak of the electroretinogram is dependent on voltage-gated calcium channels and antagonized by bestrophin (best-1). *J Gen Physiol*. 2006;127:577–589.
38. Lu H, Xi ZX, Gitajn L, Rea W, Yang Y, Stein EA. Cocaine-induced brain activation detected by dynamic manganese-enhanced magnetic resonance imaging (MEMRI). *Proc Natl Acad Sci U S A*. 2007;104:2489–2494.
39. Drapeau P, Nachshen DA. Manganese fluxes and manganese-dependent neurotransmitter release in presynaptic nerve endings isolated from rat brain. *J Physiol*. 1984;348:493–510.
40. Carlson RO, Masco D, Brooker G, Spiegel S. Endogenous ganglioside GM1 modulates L-type calcium channel activity in N18 neuroblastoma cells. *J Neurosci*. 1994;14:2272–2281.
41. Berkowitz BA, Roberts R, Penn JS, Gradianu M. High-resolution manganese-enhanced MRI of experimental retinopathy of prematurity. *Invest Ophthalmol Vis Sci*. 2007;48:4733–4740.
42. Cross DJ, Flexman JA, Anzai Y, et al. In vivo manganese MR imaging of calcium influx in spontaneous rat pituitary adenoma. *Am J Neuroradiol*. 2007;28:1865–1871.
43. Berkowitz BA, Bissig D, Bergman D, Bercea E, Kasturi VK, Roberts R. Intraretinal calcium channels and retinal morbidity in experimental retinopathy of prematurity. *Mol Vis*. 2011;17:2516–2526.
44. Rex TS, Tsui I, Hahn P, et al. Adenovirus-mediated delivery of catalase to retinal pigment epithelial cells protects neighboring photoreceptors from photo-oxidative stress. *Hum Gene Ther*. 2004;15:960–967.
45. Atalla L, Fernandez MA, Rao NA. Immunohistochemical localization of catalase in ocular tissue. *Curr Eye Res*. 1987;6:1181–1187.
46. Wangsa-Wirawan ND, Linsenmeier RA. Retinal oxygen: fundamental and clinical aspects. *Arch Ophthalmol*. 2003;121:547–557.
47. Zhi Z, Chao JR, Wietecha T, Hudkins KL, Alpers CE, Wang RK. Noninvasive imaging of retinal morphology and microvasculature in obese mice using optical coherence tomography and optical microangiography. *Invest Ophthalmol Vis Sci*. 2014;55:1024–1030.
48. Paques M, Tadayoni R, Sercombe R, et al. Structural and hemodynamic analysis of the mouse retinal microcirculation. *Invest Ophthalmol Vis Sci*. 2003;44:4960–4967.

Investigative Ophthalmology & Visual Science